Model Studies on *p*-Hydroxybenzoate Hydroxylase. The Catalytic Role of Arg-214 and Tyr-201 in the Hydroxylation Step

Robert D. Bach* and Olga Dmitrenko

Contribution from the Department of Chemistry and Biochemistry, University of Delaware, Newark, Delaware 19716

Received May 23, 2003; E-mail: del.edu

Abstract: A model C-(4a)-flavinhydroperoxide (**FlHOOH**) is described that contains the tricyclic isoalloxazine moiety, the C-4a-hydroperoxide functionality, and a β-hydroxyethyl group to model the effect of the 2′-OH group of the ribityl side chain of native FADHOOH. The electronic structures of this reduced flavin (**H$_3$Fl$_{red}$**), its N1 anion (**H$_2$Fl$_{red}$$^-$**), oxidized flavin (**HFl$_{ox}$**), and **FlHOOH** have been fully optimized at the B3LYP/6-31+G(d,p) level of theory. This model C-4a-flavinhydroperoxide is used to describe the transition state for the key step in the paradigm aromatic hydroxylase, *p*-hydroxybenzoate hydroxylase (PHBH): the oxidation of *p*-hydroxybenzoate (*p*-OHB). The Tyrosine-201 residue in PHBH is modeled by phenol, and Arginine-214 is modeled by guanidine. Electrophilic aromatic substitution proceeds by an S$_N$2-like attack of the aromatic sextet of *p*-OHB phenolate anion on the distal oxygen of **FlHOOH 3**. The transition structure for oxygen atom transfer is fully optimized [B3LYP/6-31+G(d,p)] and has a classical activation barrier of 24.9 kcal/mol. These data suggest that the role of the Tyr-201 is to orient the *p*-OHB substrate and to properly align it for the oxygen transfer step. Although the negatively charged phenolate oxygen does activate the C-3 carbon of *p*-OHB phenolate anion toward oxidation relative to *ortho* oxidation of the carboxylate anion, it appears that H-bonding the Tyr-201 residue to this phenolic oxygen stabilizes both the ground state (GS) and the transition state (TS) approximately equally and therefore plays only a minor role, if any, in lowering the activation barrier. Complexation of *p*-OHB with guanidine has only a modest effect upon the oxidation barriers. When the complex is in the form of a salt-bridge (**10a**), the barrier is only slightly reduced. When the TSs are placed in THF solvent (COSMO) with full geometry optimization, salt-bridge TS-**A** is slightly favored ($\Delta\Delta E^{\ddagger}$ = 2.3 kcal/mol).

1. Introduction

Flavoprotein monooxygenases (FMOs) are capable of catalyzing numerous oxygen atom transfer reactions. At one end of this spectrum, FMOs oxidize a wide variety of heteroatom xenobiotics, while at the other end *p*-hydroxybenzoate hydroxylase (PHBH) is essentially specific for 4-hydroxy aromatics. The paradigm FMO, PHBH, is among the most thoroughly studied enzymatic reactions and has become the model for the study of flavoprotein monoxygenases.[1] Substantial literature exists for both mechanistic[2–5] and crystallographic[6–9] studies on the PHBH-catalyzed monooxygenation of *p*-hydroxybenzoate

(*p*-OHB) to form 3,4-dihydroxybenzoate. The overall oxidative process occurs in two discrete stages. In the initial reductive half-reaction, *p*-OHB and NADPH bind to the enzyme, and NADPH reduces the FAD cofactor. In the oxidative half-reaction, reduced flavin reacts with dioxygen to form C-(4a)-flavinhydroperoxide (FlHOOH). It is this short-lived (2.5 ms)

(1) (a) Walsh, C. In *Flavins and Flavoproteins*; Vincent, M., Williams, C. H., Eds.; Elsevier/North-Holland: Amsterdam, 1982; pp 121–132. (b) Ballou, D. P. In *Flavins and Flavoproteins*; Vincent, M., Williams, C. H., Eds.; Elsevier/North-Holland: Amsterdam, 1982; p 301. (c) Bruice, T. C. In *Flavins and Flavoproteins*; Vincent, M., Williams, C. H., Eds.; Elsevier/North-Holland: Amsterdam, 1982; pp 265–277. (d) Wierenga, R. K.; Kalk, K. H.; van der Laan, J. M.; Drenth, J.; Hofsteenge, J.; Weijer, W. J.; Jekel, P. A.; Beintema, J. J.; Muller F.; van Berkel, W. J. In *Flavins and Flavoproteins*; Vincent, M., Williams, C. H., Eds.; Elsevier/North-Holland: Amsterdam, 1982; pp 11–18. (e) Bruice, T. C. In *Flavins and Flavoproteins*; Bray, R. C., Engel, P. C., Mayhew, S. G., Eds.; Walter de Gruyter: Berlin, 1984; pp 57–60. (f) Walsh, C. *Enzymatic Reaction Mechanisms*; W. H. Freemen and Co.: San Francisco, CA, 1979; pp 406–463.
(2) Ballou, D. P. In *Flavins and Flavoproteins*; Bray, R. C., Engel, P. C., Mayhew, S. G., Eds.; Walter de Gruyter: Berlin, 1984; pp 605–618.
(3) Müller, F. *Biochem. Soc. Trans.* **1985**, *13*, 443.
(4) (a) Entsch, B. *Methods Enzymol.* **1990**, *188*, 138. (b) Ortiz-Maldonado, M.; Aeschliman, S. M.; Ballou, D. P.; Massey, V. *Biochemistry* **2001**, *40*, 8705.
(5) Massey, V.; Schopfer, L. M.; Andreson, R. F. In *Oxidases and Related Systems*; King, T. E., Mason, H. S., Morrison, M., Eds.; Alan R. Liss: New York, 1988; pp 147–166.
(6) (a) Schreuder, H. A.; Van der Laan, J. M.; Hol, W. G. J.; Drenth, J. *J. Mol. Biol.* **1988**, *199*, 637. (b) Schreuder, H. A.; Prick, P. A. J.; Wierenga, R. K.; Vriend, G.; Wilson, K. S.; Hol, W. G. J.; Drenth, J. *J. Mol. Biol.* **1989**, *208*, 679.
(7) Schreuder, H. A.; Hol, W. G. J.; Drenth, J. *Biochemistry* **1990**, *29*, 3101.
(8) (a) Van der Laan, J. M.; Swarte, M. B. A.; Gronendijk, H.; Hol, W. G. J.; Drenth, J. *Eur. J. Biochem.* **1989**, *179*, 715. (b) van der Laan, J. M.; Schreuder, H. A.; Swarte, M. B. A.; Wierenga, R. K.; Kalk, K. H.; Hol, W. G. J.; Drenth, J. *Biochemistry* **1989**, *28*, 7199. (c) Schreuder, H. A.; van der Laan, J. M.; Swarte, M. B. A.; Kalk, K. H.; Hol, W. G. J.; Drenth, J. *Proteins: Struct., Funct., Genet.* **1992**, *14*, 178.
(9) (a) van Berkel, W. J. H.; Eppink, M. H. M.; Schreuder, H. A. *Protein Sci.* **1994**, *3*, 2245. (b) Schreuder, H. A.; Mattevi, A.; Obmolova, G.; Kalk, K. H.; Hol, W. G. J.; van der Bolt, F. J. T.; van Berkel, W. J. H. *Biochemistry* **1994**, *33*, 10161. (c) Lah, M. S.; Palfey, B. A.; Schreuder, H. A.; Ludwig, M. L. *Biochemistry* **1994**, *33*, 1555. (d) Jadan, A. P.; van Berkel, W. J. H.; Golovleva, L. A.; Golovlev, E. L. *Biochemistry (Moscow)* **2001**, *66*, 898. Palfrey, B. A.; Entsch, B.; Ballou, D. P.; Massey, V. *Biochemistry* **1994**, *33*, 1545.

intermediate hydroperoxide **1** that is thought to hydroxylate the substrate by transferring its OH group to the 3-position of *p*-hydroxybenzoate. The apparent facile oxidation of an aromatic ring is an interesting enigma because both experimental[10] and theoretical data[11] suggest that 4a-flavinhydroperoxides have only modest reactivity as oxygen atom donors.
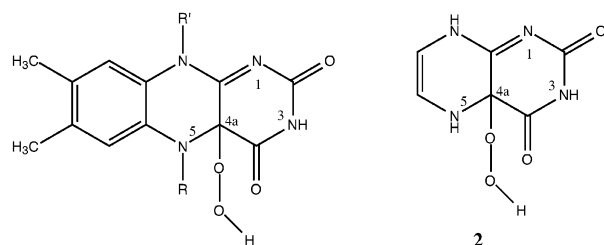
1   R'=2'- OH ribityl side chain; R=H; (FlHOOH)
1a R'= CH$_3$; R=H (Lumiflavin)
1b R'= CH$_3$; R=C$_2$H$_5$ (FlEtOOH)
3   R'= C$_2$H$_4$OH; R=H (FlHOOH **3**)

A striking feature established by X-ray analysis is the presence of a hydrogen-bonding network between the substrate and three tyrosine residues of the protein.[6b] *p*-OH-benzoate hydroxylase influences the reactivity of the substrate by modulating the pK_a of the 4-hydroxyl group of *p*-OHB by shifting the pK_a from 9.3 to 7.4.[12] Thus, it is thought that a substantial portion of the more reactive anionic form of the *p*-OHB substrate is present at physiological pH. Titration at various pH values also suggests that the observed pK_a of 7.4 for the wild-type enzyme−substrate complex is due to binding of the substrate in its phenolate form. In the final model, however, it is thought that only Tyr201 is directly H-bonded to the substrate hydroxyl group.[7] No other protein groups at the substrate-binding site with obvious catalytic capability have been identified with certainty.

It has been assumed generally that any mechanism proposed for the hydroxylation step must accommodate the observation based upon site-directed Tyr201 → Phe mutant studies that Tyr201 is an essential residue because the Phe mutant has less than 6% of the activity of the wild-type enzyme.[9c,12a] When the reduced Tyr201 → Phe *p*-hydroxybenzoate H-bonded complex reacts with oxygen, a relatively long-lived flavin-C(4a)-hydroperoxide (**1**) is formed; however, it slowly eliminates HOOH with very little substrate hydroxylation. Thus, either the flavin can hydroxylate the substrate or in an unproductive mode it can eliminate HOOH to re-form the oxidized flavin (Fl$_{ox}$).[12a]

Although the experimental evidence garnered supports the role of Tyr201 as activating the substrate by stabilizing it in the form of its phenolate anion,[12a] this long-standing assertion has come into question. Similar mutant studies were performed with Asn300 → Asp, and no ionization of mutant-bound *p*-OHB was observed up to pH 8.5.[9e] However, more recent mutant

studies,[12c] where the terminal His72 residue was changed to Asn, suggest that reduction is controlled by the protonation state of *p*-OHB and that ionization to the phenolate facilitates the movement of flavin between its so-called "in" and "out" conformations. Similarly, Pro293 → Ser mutant studies led to the suggestion that the negative charge of the phenolate oxygen of *p*-OHB is repelled by the negative charge of the peptide Pro 293 oxygen, also resulting in a conformational change.

Free energy relationships in a classical physical organic sense suggest that the mechanism of the hydroxylation step is best described as an electrophilic aromatic substitution.[13] On the basis of the spectra of substituted cyclohexadienones, Anderson et al. also suggest that a simple nucleophilic model may be correct.[14a]

On the basis of pulse radiolysis experiments, the O−O BDE of FlHO−OH has been suggested to be less than 26 kcal/mol.[14b] For a comparison, the O−O BDE (ΔH_{298}) of CH3O−OH (46.0 kcal/mol) and *t*-BuO−OH (48.3 kcal/mol) are reasonably well established.[15a] We estimate the O−O BDE in our model flavin hydroperoxide to be ∼40 kcal/mol.[11b] FlHOOH (**1**) does appear to possess thermodynamic stability when hydrogen bonded to its surrounding residues. However, in the absence of the stabilizing influence of the active site, in aqueous solution under pulse radiolysis experimental conditions, the breakdown of FlHOOH into Fl$_{ox}$ and HOOH is very rapid ($t_{1/2}$ = 2.5 ms).[16]

There have been relatively few theoretical studies aimed at the mechanism of PHBH processes. Vervoort et al.[17] have suggested on the basis of AM1 calculations that a correlation exists between ln k_{cat} for the conversion of a series of 4-hydroxylated substrates and the energy of their highest occupied molecular orbital (HOMO). This led to the suggestion that these reactions are controlled by the characteristics of their frontier molecular orbitals. Peräkylä and Pakkanen[18] studied the proton-transfer step in the *ortho*-hydroxylation of *p*-OHB. On the basis of HF/3-21G calculations, they arrived at the conclusion that the intermediate in the hydroxylation step is the radical OH adduct of *p*-hydroxybenzoate.

There have also been several attempts to define the hydroxylation step in PHBH using quantum mechanical/molecular mechanical (QM/MM) methods. Ridder et al.[19] demonstrated a correlation of calculated activation energies with experimental rate constants for an enzyme-catalyzed aromatic hydroxylation. Billeter et al.[20] studied the hydroxylation of *p*-hydroxybenzoate in its various anionic states and concluded that the dianion was the most probable form of *p*-OHB at the hydroxylation step. Both of these QM/MM studies used the closed-shell semi-

(10) (a) Ball, S.; Bruice, T. C. *J. Am. Chem. Soc.* **1979**, *101*, 4017. (b) Ball, S.; Bruice, T. C. *J. Am. Chem. Soc.* **1980**, *102*, 6498. (c) Bruice, T. C.; Noar, J. B.; Ball, S.; Venkataram, U. V. *J. Am. Chem. Soc.* **1983**, *105*, 2452. (d) Bruice, T. C. *J. Chem. Soc., Chem. Commun.* **1983**, 14. (e) Kemal, C.; Chan, T. W.; Bruice, T. C. *Proc. Natl. Acad. Sci. U.S.A.* **1977**, *74*, 405.
(11) (a) Canepa, C.; Bach, R. D.; Dmitreko, O. *J. Org. Chem.* **2002**, *67*, 8653. (b) Bach, R. D.; Dmitrenko, O. *J. Phys. Chem. B* **2003**, *107*, 12851.
(12) (a) Entsch, B.; Palfey, B. A.; Ballou, D. P.; Massey, V. *J. Biol. Chem.* **1991**, *266*, 17341. (b) Gatti, D. L.; Entsch, B.; Ballou, D. P.; Ludwig, M. L. *Biochemistry* **1996**, *35*, 567. (c) Frederick, K. K.; Ballou, D. P.; Palfey, B. A. *Biochemistry* **2001**, *40*, 3891. (d) Palfey, B. A.; Basu, R.; Frederick, K. K.; Entsch, B.; Ballou, D. P. *Biochemistry* **2001**, *40*, 8438.
(13) Ortiz-Maldonado, M. Ballou, D. P.; Massey, V. *Biochemistry* **1999**, *38*, 8124.
(14) (a) Merenyi, G.; Lind, J.; Anderson, R. F. *J. Am. Chem. Soc.* **1991**, *113*, 9371. (b) Merenyi, G.; Lind, J. *J. Am. Chem. Soc.* **1991**, *113*, 3146.
(15) (a) Estevez, C. M.; Dmitrenko, O.; Winter, J. E.; Bach, R. D. *J. Org. Chem.* **2000**, *65*, 8629. (b) Bach, R. D.; Ayala, P. Y.; Schlegel, H. B. *J. Am. Chem. Soc.* **1996**, *118*, 12758.
(16) Anderson, R. F. In *Flavins and Flavoproteins*; Bray, R. C., Engel, P. C., Mayhew, S. G., Eds.; Walter de Gruyter: Berlin, 1984; pp 57−60.
(17) Vervoort, J.; Rietjens, I. M. C. M.; van Berkel, W. J. H.; Veeger, C. *Eur. J. Biochem.* **1992**, *206*, 479.
(18) Peräkylä, M.; Pakkanen, T. A. *J. Am. Chem. Soc.* **1993**, *115*, 10958.
(19) (a) Ridder, L.; Mulholland, A. J.; Rietjens, I. M. C. M.; Vervoort, J. *J. Am. Chem. Soc.* **2000**, *122*, 8728. (b) Ridder, L.; Mulholland, A. J.; Vervoort, J.; Rietjens, I. M. C. M. *J. Am. Chem. Soc.* **1998**, *120*, 7641. (c) Ridder, L.; Palfey, B. A.; Vervoort, J.; Rietjens, I. M. C. M. *FEBS Lett.* **2000**, *478*, 197.
(20) Billeter, S. R.; Hanser, C. F. W.; Mordasini, T. Z.; Scholten, M.; Thiel, W.; van Gunsteren, W. F. *Phys. Chem. Chem. Phys.* **2001**, *3*, 688.

emperical AM1 method to study the hydroxylation step that involves O−O bond dissociation.

More recently, Canepa et al.[11a] have used density functional theory (DFT) to examine the reactivity of model bicyclic and tricyclic C-(4a)-flavinhydroxides (**2** and **3**) relative to other more commonly employed oxidizing agents such as peracids in the oxidation of dimethyl sulfide (DMS). Theoretical calculations at the B3LYP/6-31G+(d,p) level suggest that the intrinsic gas-phase reactivity of model C-(4a)-flavinperoxide **3** is about 10^9 greater than *t*-BuOOH but is still about 10^7 less reactive than peroxyformic acid toward DMS. This study has been extended to include the oxidation of a series of xenobiotics including $(CH_3)_3N$, $(CH_3)_2S$, $(CH_3)_3P$, and $(CH_3)_2Se$ by model C-(4a)-flavinhydroxide **3** at the B3LYP/6-31+G(d,p) level.[11b] The gas-phase reactivity of **FlHOOH** toward these four nucleophiles is estimated to be $10^7−10^{12}$ greater than that of *t*-BuOOH but $10^2−10^6$ less than that of peroxyformic acid. Native FADHOOH, as modeled in this work by **3**, while intermediate in reactivity between a peracid and ROOH, is still capable of enzymatically oxidizing the benzene ring in *p*-hydroxybenzoic acid.[1] It is the source of this reactivity that we strive to identify in the present study. A related question that we now address is whether the H-bonding interactions of ionized *p*-OHB with Tyr-201 actually increase the rate of hydroxylation.

2. Computational Details

Quantum chemistry calculations were carried out using the Gaussian 98 program[21] system utilizing gradient geometry optimization.[22] All geometries were fully optimized using the B3LYP functional[23,24] with 6-31G(d) and 6-31+G(d,p) basis sets. Vibrational frequency calculations at the same level of the geometry optimization were performed to characterize the stationary points as either minima or transition structures (first-order saddle point). Frequency calculations for the larger tricyclic systems were at 6-31G(d). Proton affinities (PA) were estimated by single point energy corrections (B3LYP/6-31+G(3df,2p)) on a 6-31+G(d,p) geometry with the exception of the larger systems. The PAs were estimated as differences in the total energy between the protonated and the corresponding neutral species. Inclusion of the zero-point vibrational energies (ZPVE) in estimation of the PAs systematically decreases the PA values by about 8 kcal/mol (see Supporting Information). Thus, for comparative purposes, ZPVEs were not taken into consideration for relative PA estimations. Unless specified to the contrary, all energy values quoted in the text are at the B3LYP/6-3+1G(d,p) level. Barrier heights reported herein are computed either relative to isolated reactants, that is, *p*-OHB and the oxygen atom donor, or with respect to a fully optimized prereaction gas-phase cluster.

(21) Frisch, M. J.; Trucks, G. W.; Schlegel, H. B.; Scuseria, G. E.; Robb, M. A.; Cheeseman, J. R.; Zakrzewski, V. G.; Montgomery, J. A.; Stratmann, R. E.; Burant, J. C.; Dapprich, S.; Millam, J. M.; Daniels, A. D.; Kudin, K. N.; Strain, M. C.; Farkas, O.; Tomasi, J.; Barone, V.; Cossi, M.; Cammi, R.; Mennucci, B.; Pomelli, C.; Adamo, C.; Clifford, S.; Ochterski, J.; Petersson, G. A.; Ayala, P. Y.; Cui, Q.; Morokuma, K.; Malick, D. K.; Rabuck, A. D.; Raghavachari, K.; Foresman, J. B.; Cioslowski, J.; Ortiz, J. V.; Baboul, A. G.; Stefanov, B. B.; Liu, G.; Liashenko, A.; Piskorz, P.; Komaromi, I.; Gomperts, R.; Martin, R. L.; Fox, D. J.; Keith, T.; Al-Laham, M. A.; Peng, C. Y.; Nanayakkara, A.; Gonzalez, C.; Challacombe, M.; Gill, P. M. W.; Johnson, B.; Chen, W.; Wong, M. W.; Andres, J. L.; Gonzalez, C.; Head-Gordon, M.; Replogle, E. S.; Pople, J. A. *Gaussian 98*, revision A.7; Gaussian, Inc.: Pittsburgh, PA, 1998.
(22) (a) Schlegel, H. B. *J. Comput. Chem.* **1982**, *3*, 214. (b) Schlegel, H. B. *Adv. Chem. Phys.* **1987**, *67* (Pt. 1), 249. (c) Schlegel, H. B. In *Modern Electronic Structure Theory*; Yarkony, D. R., Ed.; World Scientific: Singapore, 1995; p 459.
(23) (a) Becke, A. D. *Phys. Rev. A* **1988**, *38*, 3098. (b) Lee, C.; Yang, W.; Parr, R. G. *Phys. Rev. B* **1988**, *37*, 785.
(24) (a) Becke, A. D. *J. Chem. Phys.* **1993**, *98*, 5648. (b) Stevens, P. J.; Devlin, F. J.; Chabalowski, C. F.; Frisch, M. J. *J. Phys. Chem.* **1994**, *98*, 11623.
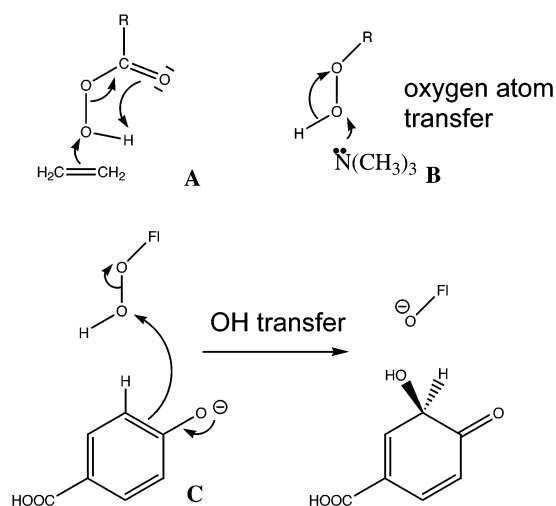
Figure 1. Mechanistic pathways for oxygen atom transfer accompanied by concerted 1,2-proton transfer (A and B) versus hydroxylation (OH transfer).
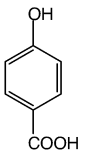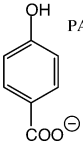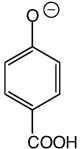
3. Results and Discussion

3.1. Electronic Factors Influencing Oxygen Atom versus Hydroxyl Transfer. Oxygen atom transfer from the −OOH moiety can, in principle, proceed by two basic pathways: (a) the formal transfer of the hydroxyl group followed by a concerted intramolecular hydrogen transfer to the departing oxyanion on the reaction coordinate or (b) a hydroxylation process where the intact OH group is transferred. The former is exemplified by the peracid epoxidation of an alkene (Figure 1, path A) that proceeds by the formal transfer of an essentially neutral OH group to the π-double bond of the alkene[25] in concert with a 1,4-proton transfer to the carbonyl oxygen of the departing carboxylate leaving group after the barrier is crossed.

Because oxygen atom transfer from a hydroperoxide most often involves a heterolytic O−O bond cleavage, the stability of the developing anionic alkoxide exerts a major influence on the position of the TS along the reaction coordinate as well as its barrier height.[11] For example, the heterolytic cleavage of the O−O bond in *t*-BuOOH affords the relatively poor *tert*-butoxide leaving group (pK_a = 19). Consequently, the S_N2-like attack on the distal oxygen by a nucleophile such as an amine is attended by a 1,2-proton transfer to the departing alkoxide that affords the neutral alcohol leaving group and the N-oxide product (Figure 1, B). The oxidation of trimethylamine by *t*-BuOOH has a very large component of 1,2-hydrogen transfer in the TS, and its imaginary frequency is 800i cm^{-1}. The extent of OH group hydrogen migration in the overall reaction vector can be determined by examining the magnitude of the single imaginary frequency for the TS. When the reaction vector is comprised mostly of light atom hydrogen migration, as in eq 1, the imaginary frequency is quite high at 1233i cm^{-1} as is the barrier height (eq 1). However, when the reaction vector is largely comprised of heavy atom OH motion as in alkene epoxidation, the single negative imaginary frequency of the first-order saddle point is much-reduced (400i−450i cm^{-1}).[11b]

(25) Bach, R. D. Peroxide Chemistry; In *DFG Research Report on Peroxide Chemistry: Mechanistic and Preparative Aspects of Oxygen Transfer*; Adam, W., Saha-Möller, C. R., Eds.; Wiley-VCH: Weinheim, 2000; pp 569−600.

Table 1. Reaction Barriers Calculated with Respect to Isolated Oxidizing Agent and Substrate[b]

substrate[a]	Oxidizing agent	$\Delta E^{\neq}$, kcal/mol	Im. freq., cm^{-1}
OH / COOH PA=338.9 / 339.9	H(C=O)OOH	18.6; **19.3**	442.1i
	MeOOH	38.9; **39.1**	469.6i
	t-BuOOH	37.8; **38.4**	454.1i
	bicyclic FlHOOH	16.5; **18.2**	416.4i
OH / COO⊖ PA=418.9 / 420.8	t-BuOOH	22.0; **24.3**	436.9i
	bicyclic FlHOOH	-2.3; **1.0**	389.2i
O⊖ / COOH PA=427.3 / 429.2	H(C=O)OOH	-1.2; **1.1**	297.9i
	MeOOH	17.5; **18.1**	443.5i
	t-BuOOH	15.5; **17.2**	423.6i
	bicyclic FlHOOH	-8.4; **-4.5**	417.2i

[a] PAs calculated in water media (COSMO) are reversed (see Supporting Information). [b] Numbers in parentheses are barriers calculated with respect to the prereaction complex. Classical activation energies ($\Delta E^{\ddagger}$) at the B3LYP/6-31G(d) level are given in plain numbers, and bold numbers correspond to B3LYP/6-31+G(d,p) calculations. The single imaginary frequency (im. freq.) of the transition structures was calculated at B3LYP/6-31G(d). Proton affinities (PA, kcal/mol) are estimated on the basis of B3LYP/6-31+G(d,p) geometries and B3LYP/6-31+G(3df,2p) single point corrections to the total energies (shown in italic style). B3LYP/6-31+G(3df,2p)//B3LYP/6-31+G(d,p) total energies of *p*-hydroxybenzoic acid, *p*-hydroxybenzoate, *p*-oxybenzoic acid anion, and *p*-oxybenzoate dianion are −496.11965, −495.56460, −495.57801, and −494.89403 au.

$$[1,2]\text{-H shift}, \quad \Delta E^{\neq} = 49.5 \text{ kcal/mol} \tag{1}$$
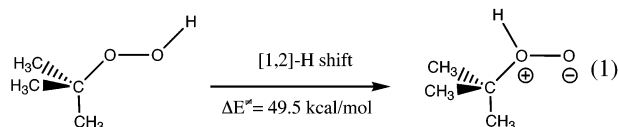
The oxidation of the aromatic ring in *p*-OHB involves initial transfer of the hydroxyl group (Figure 1, C) with a 1,2-proton shift late along the reaction pathway (see below). Such hydroxylation reactions exhibit relatively low imaginary frequencies (Table 1) in the range of 400i cm^{-1}. In particular, hydroxyl group transfer from the bi- and tricyclic FlHOOH donors produces a relatively stable alkoxide leaving group (**FlOH**, PA = 339 kcal/mol) that reduces the necessity for stabilization by the 1,2-hydrogen shift and is therefore accompanied by a lowering of the imaginary frequency (Table 1).

3.2. Oxidation versus Hydroxylation of Benzene. As part of rudimentary calculations on the PHBH mechanism, we first examine the unique oxidation of a benzene ring within the context of oxygen atom transfer versus hydroxylation. The peracid epoxidation of an alkene to an oxirane or the alkyl hydroperoxide oxidation of a heteroatom (X) to an X−O bond both involve oxygen atom transfer and by necessity either a 1,4- or a 1,2-hydrogen migration within the hydroperoxide moiety (−OOH) to form the thermodynamic O−H bond of the

leaving groups (RCOOH and ROH). In contrast, oxidation of an aromatic ring can, in principle, also proceed by hydroxyl transfer to form an intermediate hydroxylated product and a charged leaving group, RO$^-$. It has long been assumed that the PHBH oxidation of the aromatic ring in *p*-OHB involves the transfer of the intact hydroxyl group to produce, as the kinetic product, a nonaromatic hydroxylated cyclohexadienone intermediate. Very little mention has been made of the fate of the obligatory alcoholate leaving group, **FlO$^-$**.

The formal heterolytic transfer of a hydroxyl group from a hydroperoxide (ROOH) to a neutral aromatic ring can, in principle, produce an alkoxide and a hydroxylated cyclohexadienyl cation (eq 2). A fairly high activation barrier should be anticipated due to the disruption of aromaticity. Re-aromatization of this highly acidic cation should be readily achievable simply by proton (H$_a$) removal, potentially by the departing alkoxide, either in a concerted reaction or in a two-step process. However, *ortho*-hydroxylation of a phenolate anion produces a neutral hydroxylated cyclohexadienone and the alcoholate of the hydroperoxide (eq 3). The ultimate product for this anionic hydroxylation is determined by the relative stability of the two alkoxides that can potentially result from the hydroxylation step: one is the RO$^-$ of the hydroperoxide leaving group, and the other is the oxyanion of the kinetic hydroxylation product after proton transfer.

$$\tag{2}$$

$$\tag{3}$$
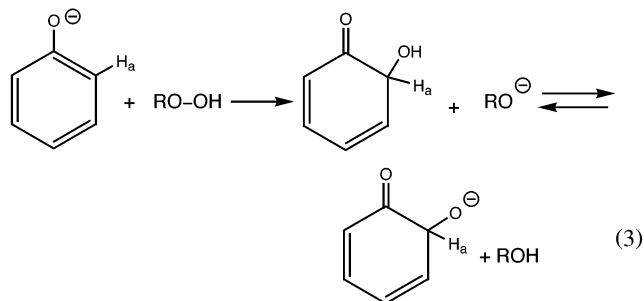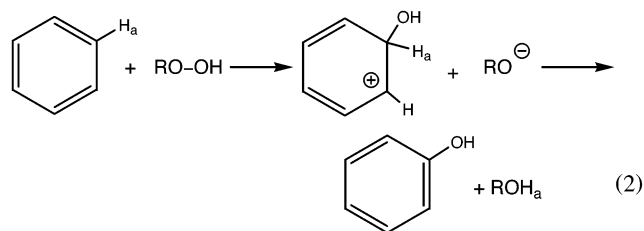
The ultimate position of the equilibrium of the OH proton in eq 3 will be determined by the proton affinity (PA) of the hydroperoxide leaving group RO$^-$ versus the PA of the hydroxylated intermediate. In most cases that we have studied, the hydroperoxide proton does a 1,2-hydrogen shift to the departing alcoholate (Figure 1, B) in concert with oxygen atom transfer at some point along the reaction coordinate as described below.

One should only expect an intact hydroxyl transfer from the −OOH moiety with highly reactive oxidants that generate very stable oxyanion leaving groups. Such an exception is the oxidation of the oxyanion of phenol with trifluoroperacetic acid (TFPA). This represents an unequivocal case where the mechanism of reaction is a two-step hydroxylation. The negative activation barrier of −15.8 kcal/mol,[26] relative to isolated

reactants, reflects the enhanced reactivity of both reacting partners. Measuring the barrier relative to a prereaction complex is complicated by the fact that the phenolate anion is sufficiently basic to abstract the peracid proton. The complexation energy of phenolate and TFPA is −38.6 kcal/mol, and the relatively high barrier (22.8 kcal/mol) with respect to the resulting H-bonded complex (phenol and $CF_3CO_3^-$) does emphasize the thermodynamic stability of the peracid oxyanion relative to the PhO^- anion (eq 4). The position of equilibrium is clearly to the right, reflecting the thermodynamic stability of the CF_3COO^- leaving group ($pK_a = 1$).

(4)

TS-4 **5**
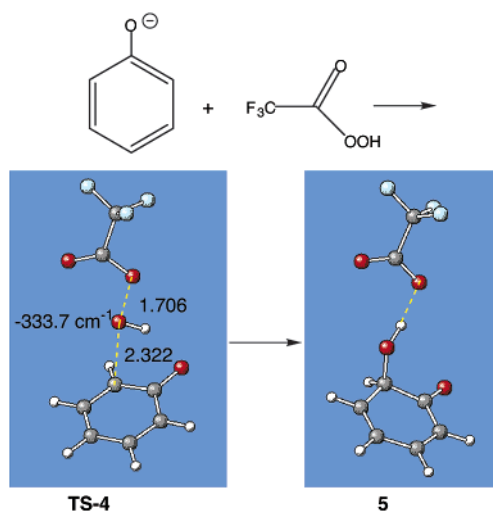
The TS for TFPA hydroxylation (TS-**4**) comes very early along the reaction coordinate (O−O = 1.706 Å; C−O = 2.322 Å), and an intrinsic reaction coordinate (IRC) analysis confirms the ultimate formation of the hydrogen-bonded complex **5** of the neutral hydroxylation product, 2-hydroxycyclohexadienone, and the trifluoroacetate anion (eq 4).

3.3. The Oxidation of *p*-Hydroxybenzoic Acid with Bicyclic Flavinhydroperoxide 2. (a) The Effect of Charge on the Barriers for *p*-OHB Oxidation. A controversial question that remains in the continuing PHBH saga is the actual degree of charge on the *p*-hydroxybenzoate substrate in the hydroxylation step. It has been most recently argued on the basis of relative activation barriers for the neutral, monoanion, and dianion, gleaned from QM/MM calculations, that the substrate exists as a dianion.[20] However, this proves to be a difficult problem to analyze because charged species typically give much lower activation barriers than their neutral counterparts (Table 1) because they are higher energy species.[11] The correct assignment of the net charge distribution is also problematic because our ability to correctly evaluate the charge distribution is not as well documented as desired and the difference between the actual charge on an atom and its formal charge can also lead to confusion.[27a]

We can demonstrate the direct effect of the net charge on the substrate on the activation barriers by comparing the

oxidation of neutral *p*-OHB to that of its respective oxyanions with a series of more typical oxidizing agents at a common level of theory (Table 1). We have employed bicyclic model flavin hydroperoxide **2** in preliminary calculations because it has been shown previously that inclusion of the third dimethylbenzene ring in FlHOOH has only a minor impact upon the relative barrier for oxygen atom transfer.[11a]

Hydroxylation of neutral *p*-OHB exhibits relatively high barriers with a series of oxidants. For example, *ortho*-hydroxylation of neutral *p*-OHB with bicyclic hydroperoxide **2** exhibited an activation barrier of 18.2 kcal/mol (eq 5), but the comparable oxidations with CH_3OOH and *t*-BuOOH had barriers twice that high (Table 1). Hydroperoxide **2**, with three electron-withdrawing substituents at C4a, exhibits reactivity toward *p*-OHB comparable to that of peroxyformic acid.


(5)
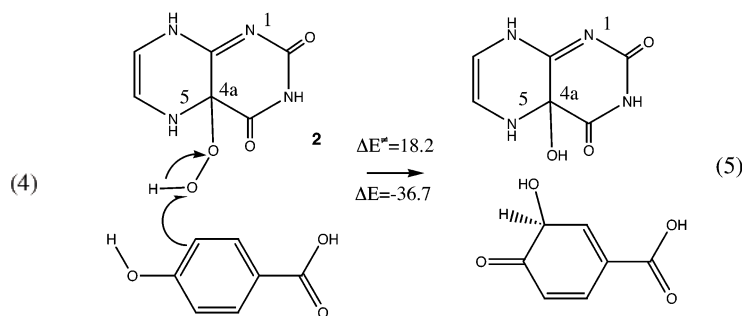
Oxidation of the corresponding monoanions, either *p*-OHB carboxylate or phenolate, gives much reduced activation barriers simply on the basis of the fact that they are higher energy anions.[11] However, the phenolate undergoes *ortho*-oxidation with **2** about 4 orders of magnitude faster ($\Delta E^\ddagger = 1.0$ versus −4.5 kcal/mol, Table 1) than oxidation of *p*-OHB carboxylate *ortho* to the neutral OH group. Oxidation of the *p*-OHB oxyanions with *t*-BuOOH also favors the phenolate over the carboxylate by 7.1 kcal/mol. These data suggest that the carbon *ortho* to the deprotonated phenol is more highly activated than the position *ortho* to the neutral OH group of the carboxylate; both substrates are monoanions that provide a more accurate comparison of the relative nucleophilicity of these two oxyanions.

In the particular case of oxygen atom transfer from bicyclic **FlHOOH 2** to neutral *p*-OHB, 1,2-proton transfer to the departing alcoholate takes place late on the reaction coordinate (eq 5). As the barriers decrease (Figure 2, TS-**6**−**8**) with increasing charge at the *ortho*-carbon, an earlier TS is observed for TS-**8** ($\Delta E^\ddagger = -4.5$ kcal/mol); the O−O distance in the TS shortens, and the developing C−O distance lengthens. Based upon recent analyses[11b] of the imaginary frequencies of such oxygen transfer reactions from ROOH, the TSs with relatively stable alcoholate RO$^-$ leaving groups should exhibit relatively low imaginary frequencies (Table 1) in the range of 400i cm^{-1}.

Oxygen atom donor **2** does produce a relatively stable alkoxide leaving group (PA = 344 kcal/mol) upon heterolytic O−O bond cleavage that lowers the energy requirements[1b] for stabilization by the 1,2-hydrogen shift to the proximal peroxide oxygen. The PA of this more stable bicyclic oxyanion is 37 kcal/mol less than that of *t*-BuO$^-$. However, in this case, the position of equilibrium is shifted to the right as exemplified above by eq 3, and the thermodynamic product is the oxyanion

(26) Negative activation barriers can be a consequence of the fact that relatively low barriers are based upon isolated reactants. When the corresponding TS is measured relative to a prereaction complex, it is typically positive.

(27) (a) Bach, R. D.; Dmitrenko, O.; Glukhovtsev, M. N. *J. Am. Chem. Soc.* **2001**, *123*, 7134. (b) Bach, R. D.; Thorpe, C.; Dmitrenko, O. *J. Phys. Chem. A* **2002**, *106*, 4325. (c) Bach, R. D.; Dmitrenko, O.; Adam, W.; Schambony, S. *J. Am. Chem. Soc.* **2003**, *125*, 924.
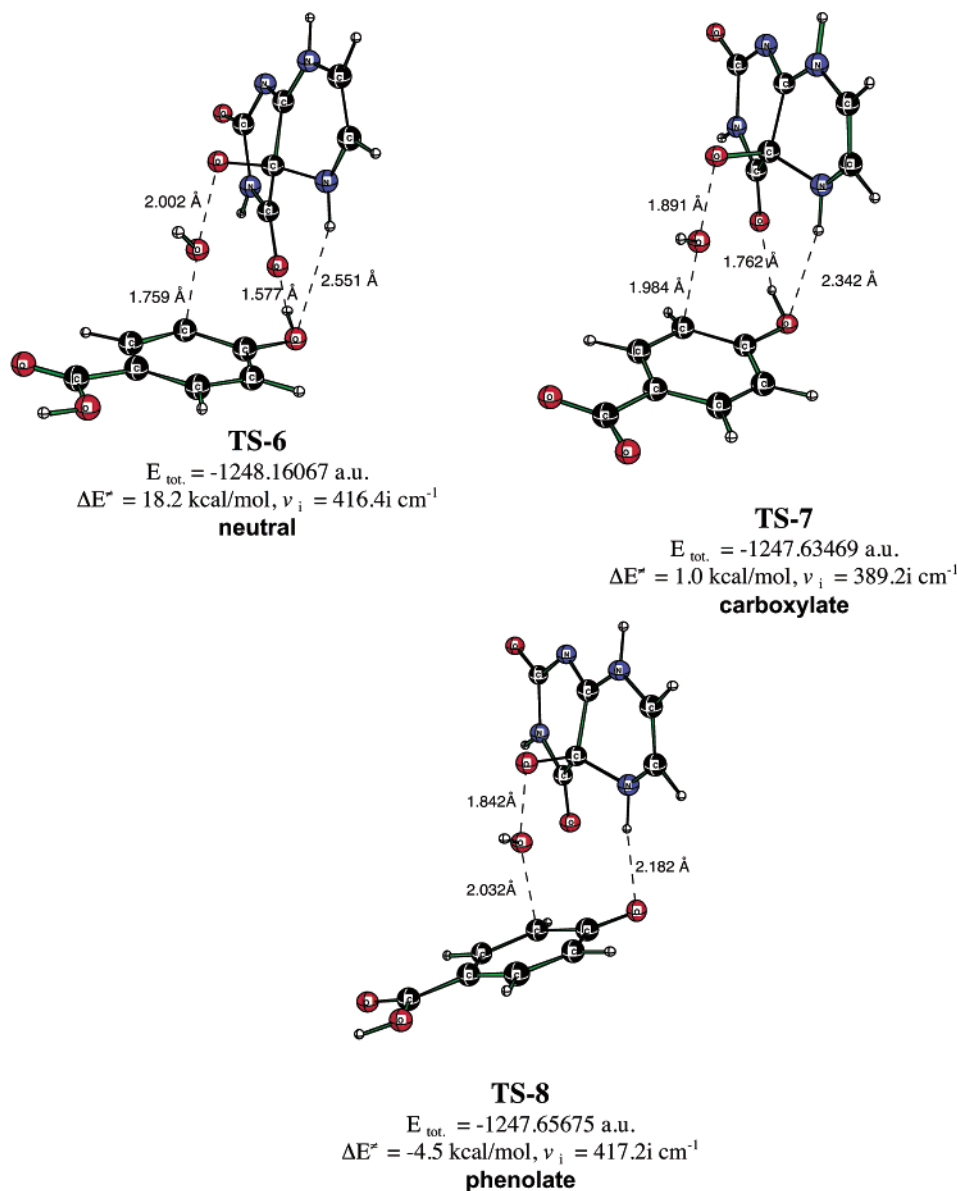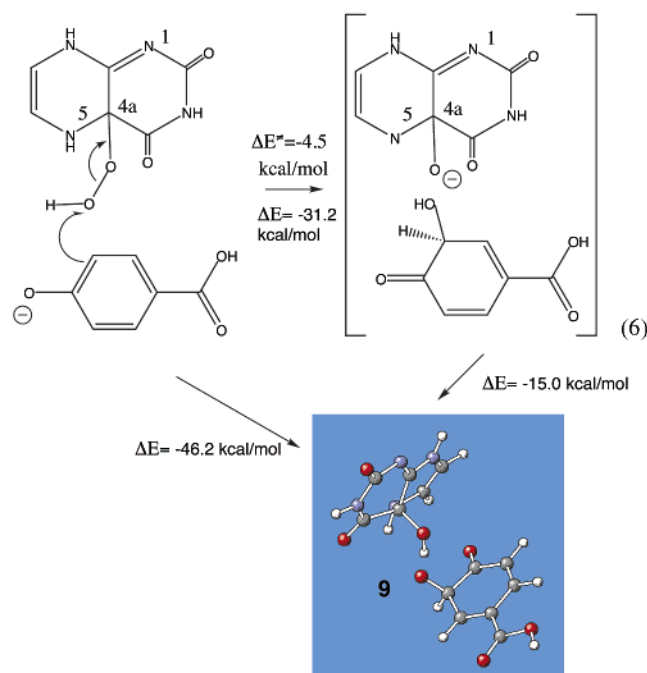
Figure 2. B3LYP/6-31+G(d,p)-optimized transition structures for the hydroxylation of *p*-hydroxybenzoic acid and its two anionic forms (carboxylate and phenolate) with model bicyclic hydroperoxide **2**. Each transition structure has a single imaginary frequency (v_i) calculated at the B3LYP//B3LYP/6-31G(d) level of theory.

of the hydroxylated *p*-OHB phenolate and the neutral **ROH** as shown in product complex **9** (eq 6). The overall oxidation is exothermic by 46.2 kcal/mol.

Hence, we propose that the −OOH hydroxyl proton is transferred to the departing RO⁻ in the same manner that most such oxygen atom transfers from ROOH take place. An intrinsic reaction coordinate (IRC) analysis of the oxidation of *p*-OHB phenolate clearly establishes an exothermic proton transfer ($\Delta E = -15.0$ kcal/mol) from the initially hydroxylated *p*-OHB phenolate to the departing bicyclic RO⁻ late on the reaction coordinate (eq 6). Thus, intact OH transfer (hydroxylation) should only be anticipated in those cases where the pK_a of the alcoholate leaving group arising from O−O bond cleavage is much lower than that of the intermediate hydroxylation product as demonstrated above for trifluoroperoxyacetic acid (eq 4). We do add the caveat that the catalytic function of an active site residue could alter the position of equilibrium of proton transfer, but no such hypothesis has been put forward to date.

(b) The Relative Stability of the Oxyanions of *p*-OHB. In general, one would anticipate that the *p*-OHB carboxylate should be more stable than the phenolate and that the higher energy of the two *p*-OHB oxyanions would exhibit the lower activation barrier for oxidation. The relative stability of the two gas-phase oxyanions can be estimated from their proton affinities (PA). The PA [B3LYP/6-31+G(3df,2p)//B3LYP/6-31+G(d,p)] of the phenolate in *p*-OHB (339.9 kcal/mol, 330.5 with ZPVE correction) is 8.6 kcal/mol lower than the carboxylate anion (348.3 kcal/mol, 338.6 with ZPVE). The PAs of the parent phenol and benzoic acid phenolate and benzoate anions [345.6 and 337.5 kcal/mol, B3LYP/6-31+G(d,p)+ZPVE] are in the anticipated order with the phenol oxyanion being more basic than the carboxylate anion of benzoic acid. We attribute the reversal with *p*-OHB to the direct conjugation of the phenolate electrons with the *p*-carboxylic acid group. Thus, the more stable gas-phase *p*-OHB phenolate oxyanion exhibits a lower activation barrier ($\Delta\Delta E^{\ddagger} = 5.5$ kcal/mol) for oxygen atom transfer, supporting

$$\Delta E^{\ddagger} = -4.5 \text{ kcal/mol}$$

$$\Delta E = -31.2 \text{ kcal/mol}$$

(6)

$$\Delta E = -15.0 \text{ kcal/mol}$$

$$\Delta E = -46.2 \text{ kcal/mol}$$

the above contention that the negatively charged phenolate oxygen does have a reasonable activating influence upon the *ortho*-phenolate oxidation rate.

The above ordering of the relative stability of the *p*-OHB oxyanions is counterintuitive because we typically anticipate the stability of their conjugate bases on the basis of the fact that a carboxylic acid ($pK_a = 4-5$) is a much stronger acid than a phenol ($pK_a = 10$). It is gratifying to note that in water solvent (COSMO solvent model) this situation is reversed and the PA of the phenolate in *p*-OHB (290.4 kcal/mol) is 7.8 kcal/mol higher than the carboxylate anion, in agreement with experiment.

Because the dianion of *p*-OHB has been invoked as the likely PHBH substrate,[20] the PAs of the gas-phase dianions of *p*-OHB are also of interest. It does, in fact, require considerable energy to remove the second proton from either *p*-OHB oxyanion (420−429 kcal/mol, Table 1). This should not be too surprising because such dianions are usually formed in the laboratory by the action of such strong bases as butyllithium. However, these are gas-phase PAs, and, as noted below, the magnitude of Coulombic interactions by adjacent ions of opposite charge can be sufficiently large to compensate for such energy differences. Obviously, the gas-phase activation barrier for the oxidation of the naked dianion of *p*-OHB would decrease even further than that of the monoanion. Because the wave functions for such doubly charged species often suffer instabilities, we have chosen (see below) to include a guanidinium counterion and attempt to evaluate the effect of charge distribution on the oxidation barriers of the monoanion.

(c) The Role of Coulombic Effects in Stabilizing the *p*-OHB Carboxylate. At the active site of PHBH, the *p*-OHB carboxylate is in close proximity to an Arg-214 residue. We estimate the potential stabilizing influence of that electrostatic interaction using guanidine as a model for Arg-214. This interaction provides a way to potentially measure the stabilization of an incipient carboxylate anion in much the same way such charges are neutralized at the active site. More specifically,

what is the effect of Arg-214 on the relative pK_a of the phenolate hydrogen, and what are the relative energies of a neutral *p*-OHB−guanidine H-bonded complex versus its corresponding zwitterionic salt-bridge structure? Surprisingly, neutral guanidine complex **10** (Table 2) is actually 5.7 kcal/mol [B3LYP/6-31+G(d,p)] less acidic than its parent *p*-OHB (Table 1). The stabilization energy of guanidine with *p*-OHB to form H-bonded complex **10** is −16.8 kcal/mol. The gas-phase H-bonded complex with the neutral form of *p*-OHB is 1.3 kcal/mol more stable than salt-bridge **10a** where the carboxyl proton is transferred to form the zwitterionic guanidinium-carboxylate salt (Figure 3).
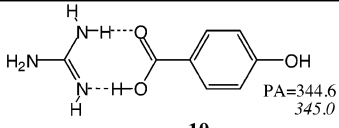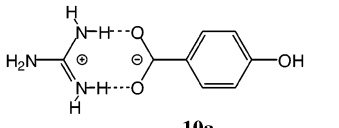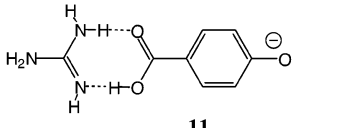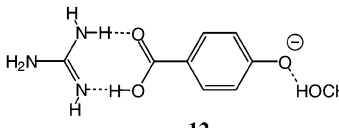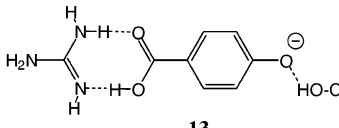
Although it is expected that the salt-bridge form **10a** is higher in energy in the gas phase, the more relevant question is as follows: what are the relative stabilities in an enzymatic environment? This point can be examined by approximating the hydrophobic environment to have a dielectric constant of 7−8. When salt-bridge **10a** is placed in THF solution (dielectric constant $\epsilon = 7.58$) using the COSMO solvent model, it is 5.8 kcal/mol lower in energy than neutral H-bonded **10**. This result is consistent with what one would anticipate at the active site where it is generally assumed that the carboxylate form is present at physiological pH. The combination/charge neutralization of gas-phase ions is typically associated with the liberation of more than 100 kcal/mol. Formation of the guanidinium salt **10a** from isolated ions, that bear a net negative charge on the *p*-OHB substrate and a positive charge on the guanidinium fragment, liberates −119.1 kcal/mol (Table 2).

The stabilization energy for complexation of guanidine with phenolate anion to produce **11** is, surprisingly, 5.4 kcal/mol less than that of neutral complex **10**. Examination of the charge distributions in H-bonded guanidine complexes **10** and **11** (Figure 3) provides a rational explanation for this observation. Although hydrogen-bonding interactions to charged species are typically much stronger than with neutrals,[27a,b] presumably, it is the increased dipole moment of **11** [most of the negative charge on phenolate complex **11** remains on the *p*-OHB fragment (0.99 e)] that is responsible for its gas-phase destabilization.

The guanidinium-carboxylate salt of **11** does not exist as a minimum in the gas phase, and when the N−H bonds are constrained to 1.04 Å as in **11a**, this structure is 15.8 kcal/mol higher in energy than mono anionic complex **11** (Figure 3). Upon release of the N−H constraints in **11a**, and geometry optimization within the COSMO solvent model (solvent = THF), it reverted to H-bonded complex **11**. When the N−H bonds are frozen in **11a**, the salt form is 3.2 kcal/mol less stable in THF than H-bonded structure **11**. Thus, in the gas phase, the salt-bridge form is always less stable than the H-bonded COOH form, while the opposite situation occurs in THF solvent (COSMO).

Complexation of *p*-OHB with guanidine has only a modest effect upon the oxidation barriers. *t*-BuOOH oxidation of neutral *p*-OHB has a barrier of 37.8 kcal/mol [Table 1, B3LYP/6-31G(d)], while oxidation in the form of its guanidinium complex, **10**, has a barrier of 35.7 kcal/mol (Table 2). When the complex is in the form of a salt-bridge (**10a**), the *t*-BuOOH barrier is only slightly reduced to 33.2 kcal/mol [B3LYP/6-31G(d)]. In the absence of a guanidine moiety, the activation

Table 2. Reaction Barriers for the Epoxidation of Differently Protonated *p*-Hydroxybenzoic Acid/Guanidine Complexes with Different Oxidizing Agents Calculated with Respect to the Isolated Oxidizing Agent and Complex[b]

substrate	Oxidizing agent	ΔE‡, kcal/mol	Im. freq., cm⁻¹
10 (PA=344.6 / *345.0*) E {complexation}[a] = -17.8 *(-16.8)*	H(C=O)OOH *t*-BuOOH	13.3 35.7	459.7i
10a E {complexation}[a] = *-119.12* kcal/mol	*t*-BuOOH	33.2; **34.5**	463.4i
11 E {complexation}[a] = -12.1 *(-11.4)*	*t*-BuOOH bicyclic FlHOOH	13.3; **15.7** -10.0; **-6.2** (25.6)	427.3i 414.6i
12 E {complexation}[a] = -27.2	bicyclic FlHOOH	-6.4; **-3.2** (26.7; **23.5**)	429.5i
13 E {complexation}[a] = -35.5	bicyclic FlHOOH tricyclic FlHOOH enzyme orientation tricyclic FlHOOH	-2.4; **0.4** (25.4; **23.3**) 1.2; **5.3** (24.6; **24.9**) -3.7; **0.6** (21.3; **20.2**)	433.1i 401.5i 419.3i

[a] Complexation energy [*E* {complexation}, kcal/mol)] is estimated with respect to isolated components at the B3LYP/6-31+G(d,p) level of theory. Italic numbers are at the B3LYP/6-31+G(3df,2p)//B3LYP/6-31+G(d,p) level. *[b]* Numbers in parentheses are barriers calculated with respect to the prereaction complex. Classical activation energies (Δ*E*‡) at the B3LYP/6-31G(d) level are given in plain numbers. Bold numbers correspond to B3LYP/6-31+G(d,p) calculations. The single imaginary frequency (im. freq.) of the transition structures was calculated at B3LYP/6-31G(d). Proton affinities (PA, kcal/mol) are estimated on the basis of B3LYP/6-31+G(d,p) geometries and B3LYP/6-31+G(3df,2p) single point corrections to the total energies (shown in italic style).

barriers for neutral *p*-OHB versus its naked carboxylate anion differ by 17.2 kcal/mol (Table 1). Thus, the description of the oxidation of this salt-bridge as an anionic oxidation is not really viable (see discussion below). The salt-bridge exerts only a modest Coulombic stabilization of the TS in gas phase.

When the two *t*-BuOOH TSs (TS-**A** and TS-**B**, Figure 4) are placed in THF solvent (COSMO) with full geometry optimization, salt-bridge TS-**A** is only slightly favored (ΔΔ*E*‡ = 2.3 kcal/mol, Figure 4).

Closer examination of the charge distributions in these transition structures shows that the net charges on the *t*-BuO⋯ OH fragments are essentially the same (−0.51 e). The net charge on the *p*-OHB fragment of "monoanion" TS-**B** is −0.59 e. When the COOH proton is transferred to the guanidine fragment in TS-**A**, its charge increases by 0.70 e which places a net charge on the *p*-OHB "dianion" fragment of −1.29 e; the overall charge on the *p*-OHB phenolate TS remains at −1 e. Thus, the

description of a dianion TS is not really correct because it refers only to the formal charge on the *p*-OHB fragment. These data do, however, tend to corroborate the earlier suggestion[20] based upon QM/MM calculations that the oxygen transfer takes place in the form of a "dianion" or a salt-bridge structure. The more significant point to be emphasized is that the position of the proton, neutral or salt-bridge, has only a modest effect upon the activation barrier for *p*-OHB oxidation (ΔΔ*E*‡ = 2.3 kcal/mol).

Finally, we address the question of the effect that hydrogen bonding of the Tyr-201 to the *p*-OHB phenolate oxygen may have on the oxidation barrier with abbreviated bicyclic model hydroperoxide **2**. Is the role of Tyr-201 to activate the substrate in the form of its phenolate anion? Using methanol as the H-bond donor, we calculate an overall stabilization energy of 27.2 kcal/mol for complex **12** (Table 2). The classical activation barrier for oxidation of *p*-OHB oxyanion-guanidine complex
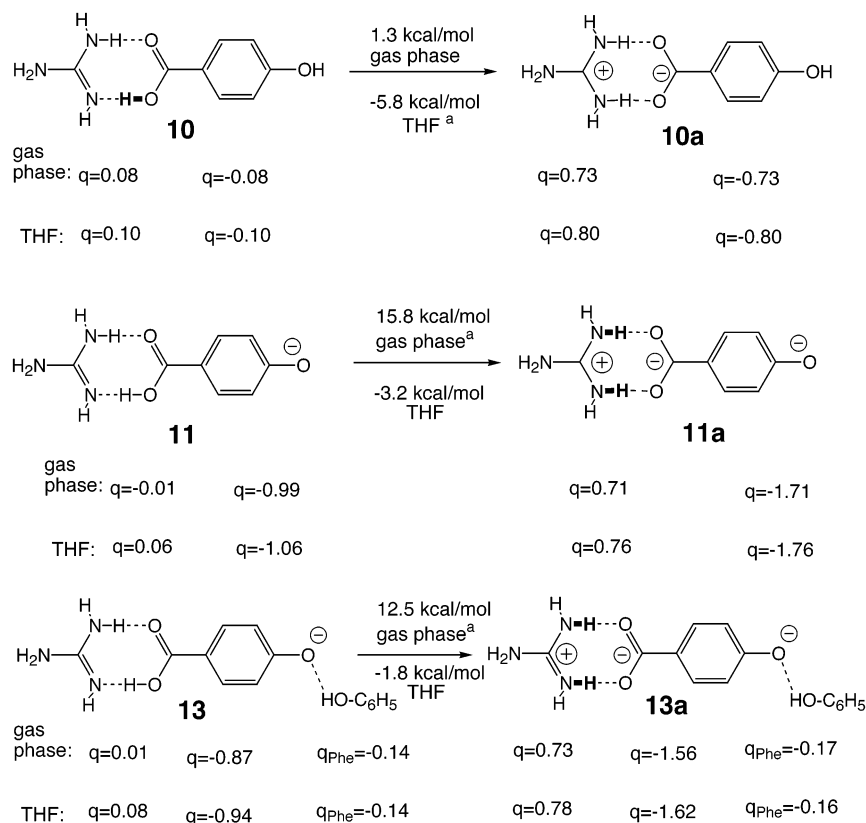
Figure 3. Energetics and charge distributions calculated at the B3LYP/6-31+G(d,p) level of theory in the gas phase and in THF solvent (COSMO) for the guanidine and *p*-OHB complexes. Charges for guanidine (q), *p*-OHB (Q), and phenol (Q_{Phe}) are calculated at the B3LYP/6-31G(d)//B3LYP/6-31+G(d,p) level of theory according to the NBO scheme. (a) At least one bond in one of the two structures, either in the gas phase or in THF solvent, is constrained (|OH| = 1.042 Å and |NH| = 1.040 Å), as indicated by bold type.

11 *ortho* to the phenolate oxygen is −6.2 kcal/mol relative to the isolated reactants **11** and **2**. The barrier for hydroxylation of phenolate complex **11** is increased from −10 to 25.6 kcal/mol [B3LYP/6-31G(d)] when measured relative to an H-bonded reactant complex of **2** and **11** (Table 2). When complex **11** is H-bonded to methanol as in **12**, this barrier is actually increased by 3.0 kcal/mol ($\Delta E^{\ddagger}$ −3.2 kcal/mol vs −6.2 kcal/mol). When this activation barrier is measured from a prereaction complex of **2** and **12**, the barrier is further increased to 23.5 kcal/mol [$\Delta\Delta E^{\ddagger}$ = 1.1 kcal/mol (B3LYP/6-31G(d), Table 2].

When phenol is used to model Tyr-201, the overall complexation energy for guanidine-phenolate-phenol complex **13** is 35.5 kcal/mol (Table 2). Comparison of this value with the complexation energies of **11** and **12** suggests a stronger H-bond strength to the phenolate oxygen in **13** than that in **12** by about 8−10 kcal/mol. The activation energy relative to isolated reactants **2** and **13** is slightly higher ($\Delta E^{\ddagger}$ = 0.4 kcal/mol) than in the case with methanol H-donor (**12**). We see no marked difference in activation barriers for all three H-bonded phenolate substrates when calculated with respect to a prereaction gas-phase complex. Thus, one may conclude that an H-bond donor (methanol or phenol) stabilizes both prereaction complex and transition structure similarly and that portends only a minor catalytic role for Tyr-201.

It is of interest to note that the salt-bridge in THF (**13a**) appears to be more stable than **13** (1.8 kcal/mol, Figure 3). Based upon the above TSs with *t*-BuOOH, these data suggest that oxidation with tricyclic flavin hydroperoxide **3** may well proceed in polar media through this "dianion" type of structure contain-

ing the salt-bridge. We reiterate that barriers calculated from a gas-phase reactant complex are always higher than those with respect to isolated reactants due to the stabilization energy of the ground-state prereaction cluster.[11] When the reaction is almost barrierless relative to its isolated reactants, as in the above case with **2**, then the marked barrier increase is due almost entirely to ground-state (GS) reactant complex stabilization.

3.4. The Electronic Structure of C-(4a)-Flavinhydroperoxide. We now extend our search for the oxygen transfer transition state using the more realistic tricyclic flavin peroxide **3**. X-ray analysis suggests that the flavin moiety is close to planarity, with reduced flavin (**H3Fl_red**) being the most planar ring system of the three flavins.[8c] The angle between the planes of the benzene ring and the pyrimidine ring is 2° for the reduced flavin, 10° for flavin in the oxidized enzyme−substrate complex, and 19° in the enzyme−product complex. However, ab initio calculations suggest a more puckered structure for the reduced flavin.[28a]

Ab initio calculations at the Hartree−Fock/6-31G* level[28a] on lumiflavin (**1a**), a 7,8-dimethylisoalloxazine with a methyl group at nitrogen 10, suggest that oxidized flavin is planar while reduced flavin is bent along the N5 and N10 axis with an angle between the benzene ring and the uracil planes of 27.3°. The ionization potentials and "butterfly" bending modes of lumiflavin (**1a**) have also been reported recently at the B3LYP/6-311G(2d,2p) level.[28b]

(28) (a) Zheng, Y.-J.; Ornstein, R. *J. Am. Chem. Soc.* **1996**, *118*, 9402. (b) Walsh, J. D.; Miller, A.-F. *J. Mol. Struct. (THEOCHEM)* **2003**, *623*, 185. (c) Zheng, Y.-J.; Ornstein, R. *J. Am. Chem. Soc.* **1996**, *118*, 11237.
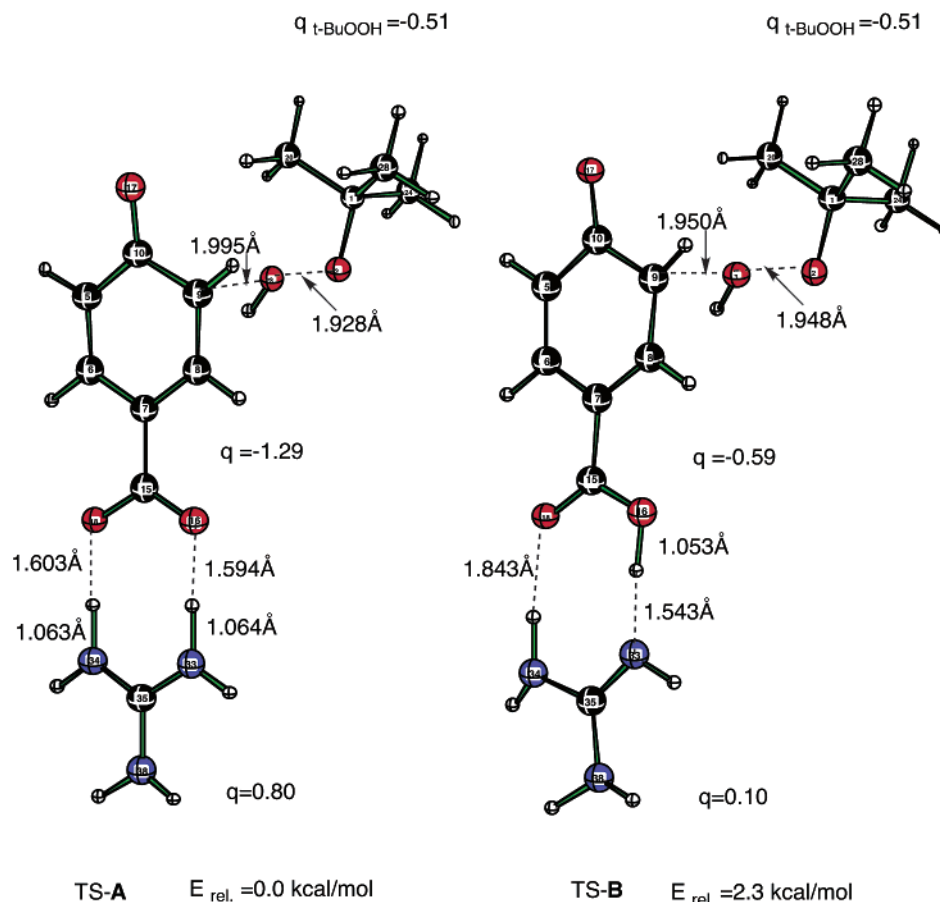
Figure 4. [B3LYP/6-31+G(d,p)+COSMO (solvent = THF)]-optimized transition structures without any geometrical constraints for the hydroxylation of dianionic-like (TS-**A**) and monoanionic-like *p*-OHB substrate (TS-**B**) with *t*-BuOOH. Charge distributions (*q*) are calculated according to the NBO scheme at the same level of theory.

In the present study, geometry optimizations were carried out using density functional theory with a relatively flexible basis set [B3LYP/6-31+G(d,p)] that includes the plus basis set that adequately treats anions and, in this case, the lone-pairs of electrons on the O−O bond. Polarization functions on hydrogen are necessary to describe hydrogen-bonding interactions. A β-hydroxyethyl group was included in minimum **3** to model the effect of the 2′-OH group of the ribityl side chain of native FADHOOH. Surprisingly little attention has been paid to a potential catalytic role for the 2′-OH group. X-ray structures, on neutral systems, typically show this hydroxyl group in the plane of the flavin ring and pointed away from the basic N_1 position. A Leu-299 residue is often shown to be within hydrogen-bonding distance of N_1 (3.1−3.5 Å between nitrogen atoms). We include the 2′-OH group in **3** to approximate the role of H-bonding interactions and their influence on the stabilization of charged species. The reduced flavin (**H₃Fl$_{red}$**) and its N_1 anion (**H₂Fl$_{red}$⁻**) are both bent, which is reflected by C6−N5−C4 and C9−N10−N1 angles given in Figure 5A. The estimated puckering angle of 24° along the N5−N10 axis is similar to one reported earlier (27.3°).[28a]

The proton affinity (PA) of **H₂Fl$_{red}$⁻** of 328.4 kcal/mol is indicative of a well-stabilized nitrogen anion. The imine nitrogen of **H₃Fl$_{red}$** at N_1 is considerably more basic than its trisubstituted nitrogen at N_5 (ΔPA = 30.3 kcal/mol).[11b] The p*K* of the reduced form would certainly be influenced by the relatively strong H-bond (1.84 Å) to N_1 shown in **H₂Fl$_{red}$⁻**. These data also

suggest that oxidized flavin (**HFl$_{ox}$**) is nearly planar (Figure 5B) with a small deviation due to the intramolecular 2′-OH···N_1 H-bond of 2.00 Å. Its hydroperoxide (**FlHOOH 3**), however, is quite puckered with a N_4−C_{4a}−C_{10a}−N_{10} dihedral angle of 41.8° (Figure 5B). While only a modest H-bond of the hydroperoxide group to the O-4 carbonyl oxygen exists in **FlHOOH 3**, its alcoholate leaving group (**FlHO⁻**, Figure 5C) appears to be effectively stabilized by an intramolecular H-bond to the 2′-OH group. The ultimate alcohol product of the oxygen transfer reaction (**FlHOH**) and its precursor alcoholate leaving group (**FlHO⁻**) are both seriously puckered, and the latter has a strong H-bond between the 2′-OH group and N_1 (1.89 Å, Figure 5C).

The experimental pK_a of 4a-FlEtOH **1b** is 9.4,[10] while the pK_a of *t*-BuOH is approximately twice that. We estimate the proton affinity of the C-4a-hydroxyflavin (**FL-OH**) derived from oxygen transfer from **3** to be 339 kcal/mol, while that of *t*-BuOH is much greater at 381 kcal/mol [B3LYP/6-31+G(d,p)]. In the oxygen transfer step, the developing oxyanion of **3** (**Fl-O⁻**) is much better stabilized as the O−O bond is cleaved than is *t*-butoxy anion, and this is clearly reflected in their difference in activation energies for the N-oxidation of trimethylamine (ΔΔ$E^{\ddagger}$ = 16.7 kcal/mol).[11a]

3.5. The Oxidation of *p*-Hydroxybenzoic Acid with C-(4a)-Flavinhydroperoxide (3). (a) The Potential Role of Tyr-201 in Activating the *p*-OHB Substrate. Computational studies of enzyme reactions have recently been greatly assisted by such
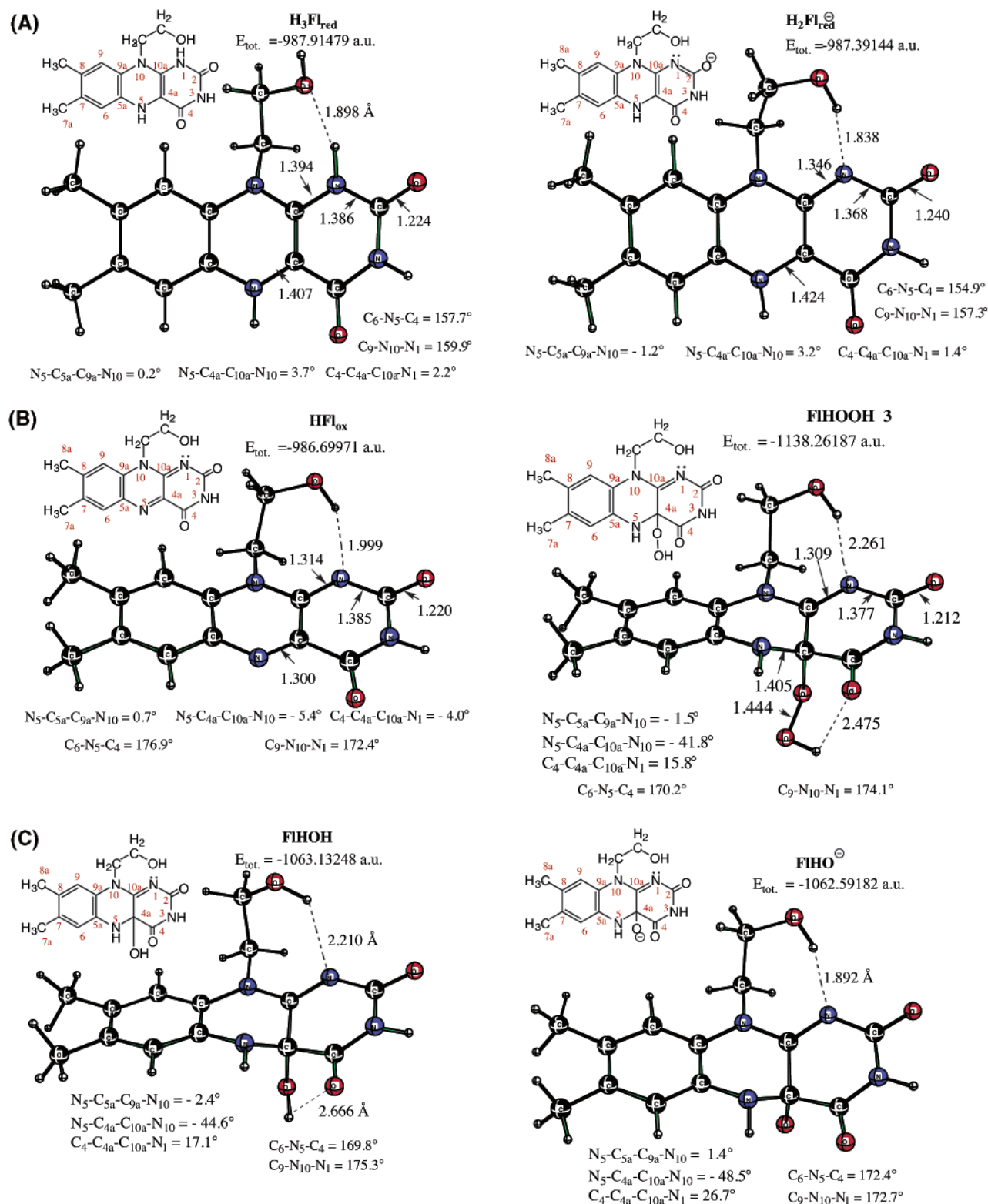
Figure 5. (A) Reduced flavin (**H₃Flᵣₑд**) and its N₁ anion (**H₂Flᵣₑд⁻**) optimized at the B3LYP/6-31+G(d,p) level of theory. (B) Oxidized flavin (**HFlₒₓ**) and its hydroperoxide (**FlHOOH 3**) optimized at the B3LYP/6-31+G(d,p) level of theory. (C) Alcohol product of the oxygen atom transfer reaction (**FlHOH**) and its intermediate alcoholate leaving group (**FlHO⁻**) optimized at the B3LYP/6-31+G(d,p) level of theory.

theoretical procedures as quantum mechanical/molecular mechanical (QM/MM) and quantum mechanical-free energy (QM-FE) methodologies.[29] Such semiempirical methods offer the advantage of treating the active-site residues within a QM framework and the surrounding protein environment by mo-

lecular mechanic or force field methods. However, when the key enzymatic reaction involves oxygen−oxygen bond rupture in the rate-limiting step, electron correlated levels of theory are required to adequately describe the energetics of O−O bond cleavage.[11b] The report of several QM/MM studies on *p*-

hydroxybenzoate hydroxylase, where the oxygen transfer step from 4a-flavin hydroperoxide to *p*-hydroxybenzoate was treated at the AM1 level,[18,19] was recently questioned.[11b] A disadvantage of this protocol is that the transition structures in the QM portion of the potential energy surface (PES) are approximated by successive elongation of the O—O bond (and formation of the developing C—O bond). In the present study, we are able to locate the transition structure for oxygen atom transfer by gradient optimization and verify the TS to be a first-order saddle point by carrying out a frequency calculation. The disadvantage of our approach is that we have included only two of the primary active site residues.

It is generally assumed that oxidation of the aromatic ring in *p*-OHB produces the hydroxylated cyclohexadienone tautomeric intermediate shown in eq 7.

(7)
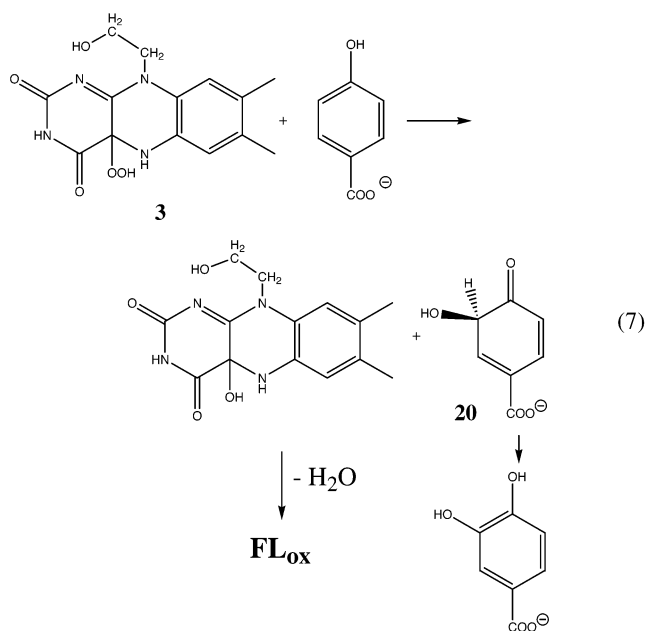
The two primary active site residues involved in the hydroxylation step in PHBH have been assigned to Tyr-201 and Arg-214. In this series of calculations, guanidine is included to model the role of Arg-214 and to maintain a net charge of −1 on the overall complex. Phenol is used to model Tyr-201, and it is H-bonded to *p*-OHB to examine its effect on the activation barrier for hydroxylation of *p*-OHB with **FlHOOH 3**. One of the problems associated with this type of enzyme modeling approach is that the model amino acid residues are not geometrically constrained by the interacting environment of the active site. A second difficulty is accurately measuring the influence of hydrogen bonding and Coulombic interactions in the ground state versus the transition state.

First, we examine the energetic consequences of hydroxylation of a neutral model complex **14** consisting of guanidine, phenol, and *p*-OHB (Figure 6). As noted above, hydroxylation

(29) (a) Field, M. J. *J. Comput. Chem.* **2002**, *23*, 48. (b) Bruice, T. C.; Kahn, K. *Curr. Opin. Chem. Biol.* **2000**, *4*, 540. (c) For a comparison of quantum mechanical/molecular mechanical (QM/MM) and quantum mechanical-free energy (QM-FE) methodologies, see: (i) CHARMM version 24bl, 1995; Prof. M. Karplus, Department of Chemistry, Harvard University, 12 Oxford Street, Cambridge, MA 02138. (ii) Gunsteren, W. F. van; Billeter, S. R.; Eising, A. A.; Hunenberger, P. H.; Kruger, P.; Mark, A. E.; Scott, W. R. P.; Tironi, I. G. *Biomolecular Simulation: The GROMOS96 Manual and user Guide*; Biomos b. v.: Zurich and Groningen, 1996.
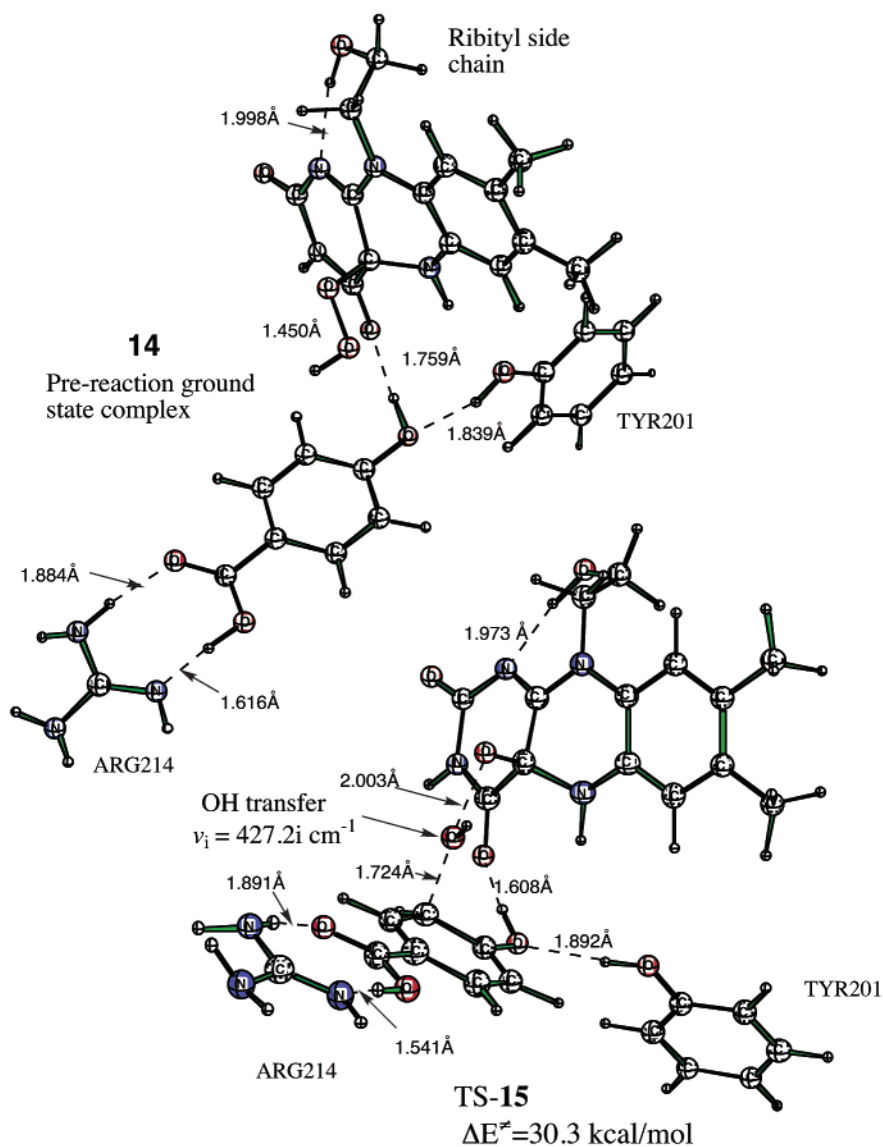
of neutral *p*-OHB itself, with bicyclic hydroperoxide **2**, has a barrier of 18.2 kcal/mol (eq 5). This barrier provides a benchmark against which we can assess the role of H-bonding of these two local residues on the hydroxylation barrier. The marked effect on increasing the barrier with respect to GS complexes with **2** (Table 2) prompted a similar exercise with **FlHOOH 3**. We address the question of the stabilizing influence of a neutral Tyr-201 on both the GS and the TS. When the COOH group of *p*-OHB is complexed to guanidine (Arg-214) and the OH moiety is H-bonded to phenol (Tyr-201), the overall stabilization energy for prereaction complex **14** (Figure 6) with respect to the four isolated fragments (including **FlHOOH 3**) is 42.1 kcal/mol [6-31G(d)]. This is a rather loose complex with a distance of 3.24 Å between the distal oxygen of **FlHOOH 3** and the *ortho* C-3 *p*-OHB carbon atom. As we typically observe, the activation barrier [TS-**15**, 30.3 kcal/mol, 6-31G(d)] for hydroxylation of this complex is markedly increased when measured relative to a stabilized ground-state cluster. Oxygen transfer comes fairly late along the reaction coordinate with an O—O distance of 2.003 Å and a developing C—O distance of 1.724 Å. The O—O—C angle is 122.5° in complex **14** and 171.3° in TS-**15**. This is a typical S_N2-like attack by the C-3 *p*-OHB carbon on the distal oxygen of **FlHOOH 3**. The gas-phase TS has the guanidine H-bonded to the COOH of *p*-OHB, and the phenol is H-bonded to the OH group of *p*-OHB in this overall neutral substrate complex. The additional stabilization of the guanidine and phenol fragments has increased the activation barrier from 18.2 kcal/mol for neutral *p*-OHB (with **2**, eq 5) to 30.3 kcal/mol.

Because we have shown that B3LYP barriers are quite reliable for this type of oxygen transfer reaction,[11,27c] an activation barrier of this magnitude would be prohibitive. It is difficult to see how additional H-bonding interactions could significantly lower this barrier. We, therefore, discount the involvement of an overall neutral immediate environment surrounding *p*-OHB in native FADHOOH.

Next, we examine the effect of the two H-bonding residues upon the oxidation barrier of the monoanion that has a formal negative charge on the phenolate oxygen of *p*-OHB. When phenol is H-bonded to *p*-OHB phenolate complex **13**, the overall complexation energy from isolated reactants (guanidine, *p*-OHB, and phenol) is 35.5 kcal/mol (Table 2). Because the complexation energy of *p*-OHB phenolate-guanidine complex **11** is 12.1 kcal/mol, this suggests that the ionic H-bond strength of phenol with the *p*-OHB phenolate oxygen is about 20−25 kcal/mol. Most of the negative charge still remains on the *p*-OHB phenolate fragment because the negative charge acquired by the H-bond donor phenol fragment in complex **13** is only 0.118 e (Figure 3). Although the complexation energy for reactant complex **13** (Table 2) is 35.5 kcal/mol, the overall stabilization energy for prereaction complex **16** H-bonded to **FlHOOH 3** is 55.1 kcal/mol (Figure 7). Despite the strength of these ionic H-bonds, this complexation energy can only serve to diminish the activation barrier if the TS is stabilized more than the GS.

In reactant complex **16**, the Tyr-201 residue is aligned with the *o*-dimethylbenzene ring, and the *p*-OHB phenolate oxygen is pointed toward the N_5 nitrogen atom of the flavin. The two additional ionic H-bonds to the *p*-OHB phenolate oxygen (to OOH and NH) add ca. 20 kcal/mol to the GS stabilization. The

Figure 6. B3LYP/6-31G(d) prereaction complex and TS with the neutral *p*-OHB substrate internally H-bonded to O=C4 of **FlHOOH**.
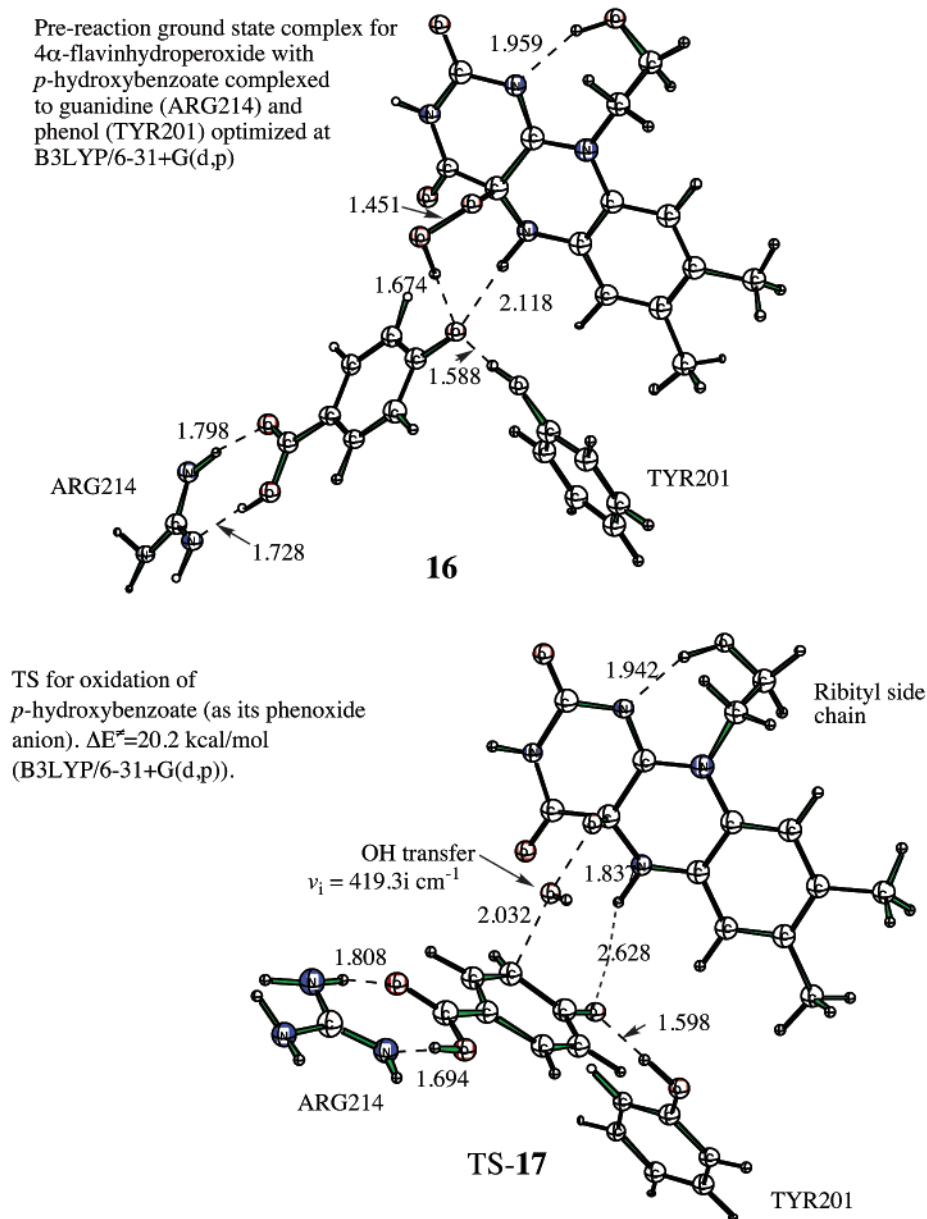
activation barrier for oxidation of this phenolate complex is 20.2 kcal/mol (TS-**17**, Figure 7) measured relative to H-bonded complex **16**. While this barrier is much lower than that for the neutral TS-**15** (30.3 kcal/mol), this is still a relatively high barrier for a negatively charged TS when compared to the barrier for oxygen atom transfer to naked oxyanion **11** (−4.5 kcal/mol, Table 2) in the absence of either H-bonding interaction. We again emphasize the point that when GS stabilization is both large and comparable to TS stabilization, then the activation barrier will be higher than that anticipated for an enzymatic reaction. This is to be expected for such a TS because the charge separation in the TS is essentially restricted to O−O bond elongation.

(b) Orientation of the *p*-OHB Substrate at the Active Site. While location of a transition structure of this complexity was quite gratifying, we soon discovered that gradient optimization, while leading us to the lowest energy TS, is not always a fruitful exercise. The orientation of the *p*-OHB with respect to the **FlHOOH** in TS-**17** was opposite to that in the X-ray structure where the Arg-214 residue is under the *o*-dimethylbenzene ring.[6−9]

Rotation of the substrate in complex **16** by approximately 180° gave prereaction complex **18** (Figure 8) that has an overall stabilization energy of 53.4 kcal/mol relative to isolated reactants. The activation barrier for hydroxylation of **18** with the local model residues now in the proper orientation with respect to the *p*-OHB substrate (TS-**19**) has increased from 20.2 (TS-**17**) to 24.9 kcal/mol. The NH hydrogen bond is no longer possible in this orientation.

The single imaginary frequency of 401.5i cm^{-1} is consistent with oxygen transfer early on the reaction coordinate as suggested by an O−O distance of 1.836 Å. In this gas-phase TS-**19**, the net charge on the *p*-OHB phenolate monoanion fragment is 0.5 electrons, and the charge on the transferring OH group is only −0.058. We do not observe migration of the COOH proton to form the zwitterionic salt-bridge structure. This orientation of the substrate complex suggested that the lower energy TS for the hydroxylation step (TS-**17**) was not the most favorable orientation for the overall reaction sequence starting with the oxidized flavin (**HFl$_{ox}$**). Because this is a multistep process, this orientation could be more favorable for an earlier step in the overall oxidative sequence starting with oxidized

Pre-reaction ground state complex for
4α-flavinhydroperoxide with
p-hydroxybenzoate complexed
to guanidine (ARG214) and
phenol (TYR201) optimized at
B3LYP/6-31+G(d,p)

1.959

1.451

1.674

2.118

1.588

1.798

ARG214

TYR201

1.728

16

TS for oxidation of
p-hydroxybenzoate (as its phenoxide
anion). $\Delta E^{\ddagger} = 20.2$ kcal/mol
(B3LYP/6-31+G(d,p)).

Ribityl side
chain

1.942

OH transfer

$\nu_i = 419.3i$ cm^{-1}

1.83

2.032

2.628

1.808

1.598

1.694

ARG214

TS-17

TYR201

Figure 7. Prereaction complex and TS with the opposite orientation of the *p*-OHB substrate as compared to the enzyme X-ray structure.

flavin. The magnitude of the barrier for anionic TS-**19** (Figure 8) suggests that the role of the Tyr-201 is to orient the *p*-OHB substrate and to properly align it for the oxygen transfer step. Although the negatively charged phenolate oxygen does activate the C-3 carbon of *p*-OHB phenolate anion toward oxidation relative to *ortho* oxidation of the carboxylate anion ($\Delta E^{\ddagger} = 1.0$ versus -4.5 kcal/mol, Table 1), it appears that H-bonding the Tyr-201 residue to this oxygen stabilizes both the GS and the TS and therefore plays only a minor role, if any, in lowering the activation barrier. The above data with hydroperoxide **2** suggest that model Arg-214 plays only a modest role in lowering the barrier for oxidation (Table 2). It has been recognized for some time that neutral conventional hydrogen-bonded acid/amine complexes are preferred in the gas phase but that the barrier for conversion to the zwitterionic salt-bridge form is small.[28c] Thus, we suggest that it is the collective interactions of many active-site residues that constitute the overall PHBH catalytic effect and that we must seek additional interactions to

lower that barrier further into the accepted experimental range of 12 kcal/mol.[30]

Conclusions

(a) These B3LYP data suggest that C-(4a)-flavinhydroperoxide (**FlHOOH 3**) is quite puckered with a $N_4-C_{4a}-C_{10a}-N_{10}$ dihedral angle of 41.8°. The ultimate alcohol product of the oxygen transfer reaction (**FlHOH**) and its precursor alcoholate leaving group (**FlHO$^-$**) are also both seriously puckered, and the latter has a strong H-bond between the 2′-OH group and N_1 (1.89 Å).

(b) The oxidation of the oxyanion of phenol with trifluoroperacetic acid represents an unequivocal case where the mechanism of reaction is a two-step hydroxylation. However, oxidation of *p*-OHB phenolate with bicyclic **FlHOOH 2** is an

(30) (a) van Berkel, W. J. H.; Muller, F.; Jekel, P. A.; Weijer, W. J.; Schreuder, H. A.; Wierenga, R. K. *Eur. J. Biochem.* **1988**, *176*, 449. (b) van Berkel, W. J. H.; Muller, F. *Eur. J. Biochem.* **1989**, *179*, 307.
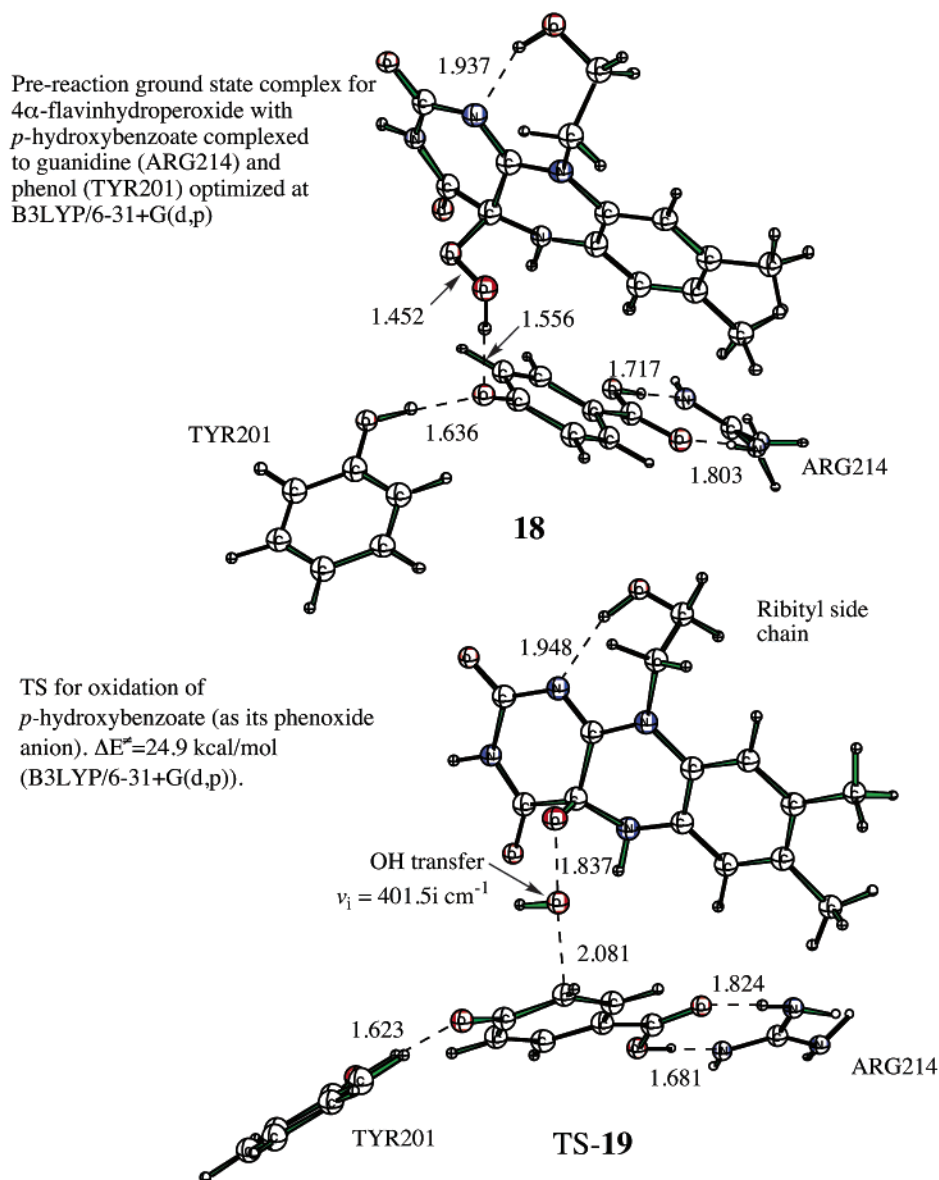
Figure 8. Prereaction complex and TS with the "natural" (enzymatic) orientation of the *p*-OHB substrate with respect to the **FlHOOH**.

oxygen atom transfer reaction with 1,2-proton transfer from the kinetic structure on the reaction pathway to the departing alcoholate. An intrinsic reaction coordinate (IRC) analysis of the oxidation of *p*-OHB phenolate clearly establishes an exothermic proton transfer ($\Delta E = -15.0$ kcal/mol) from the initially hydroxylated *p*-OHB phenolate to the departing bicyclic RO^-. We propose that the hydroxyl proton is transferred to the departing RO^- in the same manner that most such oxygen atom transfers from ROOH take place.

(c) Oxidation of *p*-OHB monoanions, either *p*-OHB carboxylate or phenolate, with bicyclic flavinhydroperoxide **2** gives much reduced activation barriers relative to neutral *p*-OHB simply on the basis of the fact that they are higher energy anions. The phenolate undergoes *ortho*-oxidation with **2** about 4 orders of magnitude faster than oxidation of *p*-OHB carboxylate *ortho* to the neutral OH group.

(d) Complexation of *p*-OHB with guanidine has only a modest effect upon the oxidation barriers. When the complex is in the form of a salt-bridge (**10a**), the barrier is only slightly reduced. When the TSs are placed in THF solvent (COSMO) with full geometry optimization, salt-bridge TS-**A** is favored ($\Delta\Delta E^{\ddagger} = 2.3$ kcal/mol).

(e) Prereaction complex **18** (Figure 8) has an overall stabilization energy of 53.4 kcal/mol relative to isolated reactants. The activation barrier for oxidation of **18** (TS-**19**) is 24.9 kcal/mol. The single imaginary frequency of 401.5i cm^{-1} is consistent with oxygen atom transfer early on the reaction coordinate to a relatively stable alcoholate leaving group (**FlO$^-$**). The magnitude of the barrier for anionic TS-**19** suggests that the role of the Tyr-201 is to orient the *p*-OHB substrate and to properly align it for the oxygen transfer step. Although the negatively charged phenolate oxygen does activate the C-3 carbon of *p*-OHB phenolate anion toward oxidation relative to *ortho* oxidation of the carboxylate anion, it appears that H-bonding the Tyr-201 residue to this phenolic oxygen stabilizes both the GS and the TS and therefore plays only a minor role, if any, in lowering the activation barrier.

Supporting Information Available: Cartesian coordinates of **HFl$_{ox}$**, **FlHOH**, **FlHO$^-$**, **H$_2$Fl$_{red}^-$**, **H$_3$Fl$_{red}$**, **FlHOOH**, and ***p*-OHB**, and different forms/complexes and TSs are shown in the figures. PAs estimated at different levels of theory in the gas phase and in water. Total energies (au) of the intermediates and products of the hydroxylation/oxygen transfer reactions calculated at the B3LYP level of theory using different basis sets (Table S1) (PDF). This material is available free of charge via the Internet at http://pubs.acs.org.

JA036310+